

Crystal structure and UV spectra of a 1,2-disubstituted benzimidazolium chloride

Tuhin Khan,* Navneet Mishra, Darshan S. Mhatre and Anindya Datta

Department of Chemistry, Indian Institute of Technology Bombay, Mumbai 400 076, India. *Correspondence e-mail: tuhin@chem.iitb.ac.in

Received 13 June 2017

Accepted 3 July 2017

Edited by A. V. Yatsenko, Moscow State University, Russia

Keywords: crystal structure; benzimidazole; hydrogen bonding; Hirshfeld surface analysis; DFT calculations; UV spectra.

CCDC reference: 1548944

Supporting information: this article has supporting information at journals.iucr.org/e

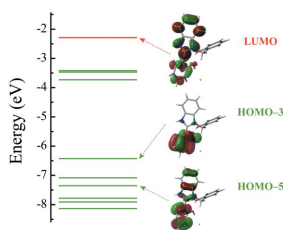
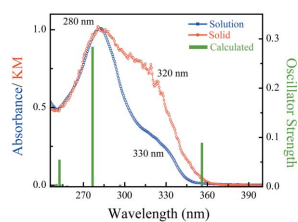
1-(2-Hydroxybenzyl)-2-(2-hydroxyphenyl)-1*H*-benzimidazol-3-ium chloride, $C_{20}H_{17}N_2O_2^+ \cdot Cl^-$, was prepared by reaction of salicylaldehyde with *o*-phenylenediamine in the presence of trimethylsilyl chloride acting as a source of HCl. As a result of steric hindrance, the cation in the crystal is far from planar: the benzimidazole ring system makes dihedral angles of 55.49 (9) and 81.36 (8)° with the planes of the phenolic groups. The crystal packing is dominated by O—H...Cl and N—H...Cl hydrogen bonds, which link the cations and anions into four-membered rings and then into chains along [100]. The title compound exhibits two transitions in the UV region, which are revealed in the solid state and solution spectra as an absorption maximum at 280 nm and a shoulder at 320 nm. According to the results of TD-DFT calculation, both transitions have a π – π^* nature and the molecular orbitals involved in these transitions are mostly localized on the benzimidazole ring system and on the phenyl ring attached to it at the 2-position.

1. Chemical context

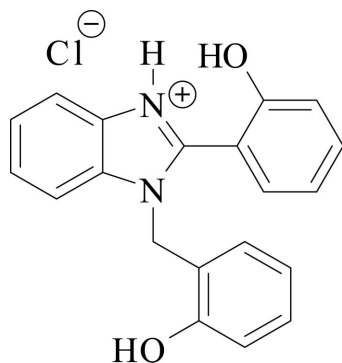
Benzimidazole derivatives are well known to exhibit antibacterial, antimalarial and anti-inflammatory properties (Keri *et al.*, 2015; Carvalho *et al.*, 2011). Besides this, 1,2-disubstituted benzimidazoles are used as intermediates in synthesis of dyes and pigments (Carvalho *et al.*, 2011). Some substituted benzimidazoles, *e.g.* 2-(2'-hydroxyphenyl)benzimidazole and its derivatives, are strongly fluorescent and show dual emission due to the excited state proton transfer (Douhal *et al.*, 1994). In the solid state, these compounds exhibit fluorescence, which is governed by their polymorphism and steric effects (Konoshima *et al.*, 2012; Benelhadj *et al.*, 2013; Shida *et al.*, 2013). Thus, this class of compounds is considered for applications in fluorescence imaging and optoelectronics (Zhao *et al.*, 2011). Benzimidazolium salts attract attention due to their non-linear optical properties (Sun *et al.*, 2011; Wang *et al.*, 2011). 2-(2'-Hydroxyphenyl)benzimidazole, which is a member of this class of compounds, exhibits rotamerism (Ríos Vazquez *et al.*, 2008). In this work, the crystal structure of 1-(2-hydroxybenzyl)-2-(2-hydroxyphenyl)-1*H*-benzimidazol-3-ium chloride and its UV spectra have been reported. DFT calculations were carried out to study the geometry and electronic transitions.

2. Structural commentary

All bond lengths and bond angles are within the ranges reported for similar structures (Ha, 2012). The asymmetric unit, consisting of a 1-(2-hydroxybenzyl)-2-(2-hydroxyphenyl)-



yl)-1*H*-benzo[*d*]imidazol-3-ium cation and a chloride anion, is presented in Fig. 1. As a result of steric hindrance, the cation is far from planar: the benzimidazole ring system makes dihedral angles of 55.49 (9) and 81.36 (8)° with the planes of phenolic groups immediately attached to it at position 2 and linked via the methylene bridge to position 1, respectively. The deviation from planarity in the 2-(2-hydroxyphenyl)benzimidazolium skeleton is larger than in the reported similar structures (Al-Douh *et al.*, 2009*b*; Wang *et al.*, 2011).



3. Supramolecular features

In the crystal, each cation forms three hydrogen bonds, two O—H···Cl and one N—H···Cl (Table 1), to chloride anions. As a result of these interactions, the cations and anions form ribbons along [100], which consist of centrosymmetric four-

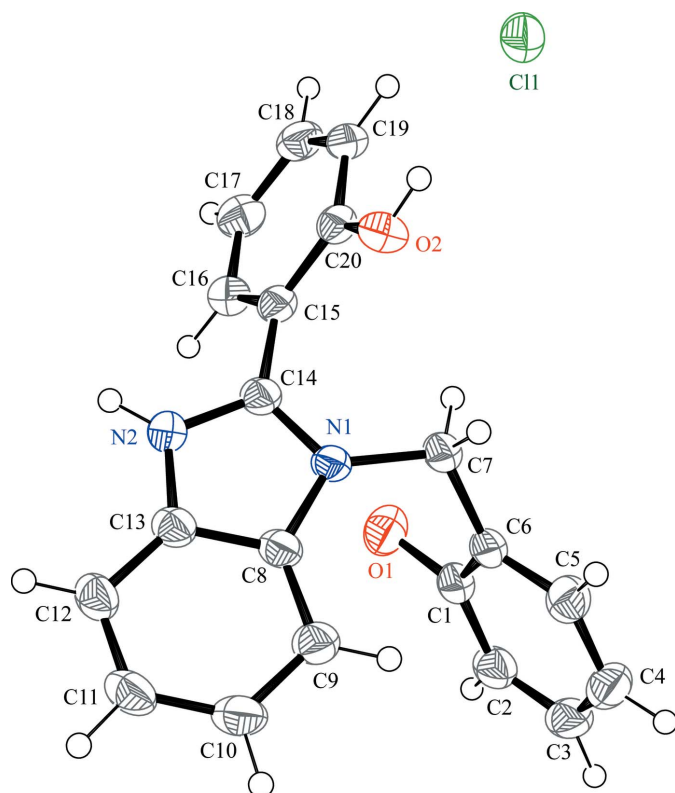


Figure 1
ORTEP diagram of the title compound with displacement ellipsoids drawn at the 50% probability level.

Table 1
Hydrogen-bond geometry (Å, °).

<i>D</i> —H··· <i>A</i>	<i>D</i> —H	H··· <i>A</i>	<i>D</i> ··· <i>A</i>	<i>D</i> —H··· <i>A</i>
O1—H1···Cl1 ⁱ	0.84	2.24	3.066 (2)	169
O2—H2···Cl1	0.84	2.23	3.071 (1)	177
N2—H2A···Cl1 ⁱⁱ	0.88	2.23	3.084 (2)	162
C16—H16···O1 ⁱⁱⁱ	0.95	2.57	3.253 (2)	129
C19—H19···Cl1	0.95	2.93	3.646 (2)	134
C7—H7B···Cg(C1-C6) ^{iv}	0.99	2.77	3.500 (2)	131

Symmetry codes: (i) $x + 1, y, z$; (ii) $-x, -y + 1, -z + 1$; (iii) $-x + 1, -y + 1, -z + 1$; (iv) $-x + 1, -y + 1, -z + 2$.

membered rings each formed by two cations and two anions in the $R_4^2(16)$ and $R_4^2(20)$ manner, as shown in Fig. 2. Some weak contacts C—H···O, C—H···Cl and C—H··· π are also present (Table 1).

4. Hirshfeld surface analysis

To evaluate the effect of close range interactions and compare their significance, Hirshfeld surface analysis (Spackman & Jayatilaka, 2009; Soman *et al.*, 2014) has been performed and its results are presented in Fig. 3. Four red spots on the Hirshfeld surface indicate short contacts. All close interactions are mediated by Cl[−] anions. The H···H and C···H interactions are associated with 46% and 26% surface area, respectively. The contributions of the Cl···H (15%) and O···H (6%) interactions are smaller, but significant for the crystal architecture.

5. Quantum chemical calculation

The geometry of the cation–anion pair in the gas phase was optimized with density functional theory (DFT) using GAUSSIAN09 package (Frisch *et al.*, 2009) within the framework of B3LYP/6-31G(d). Frequency calculations were carried out to confirm that the structure corresponds to a minimum. The optimized bond lengths agree with those

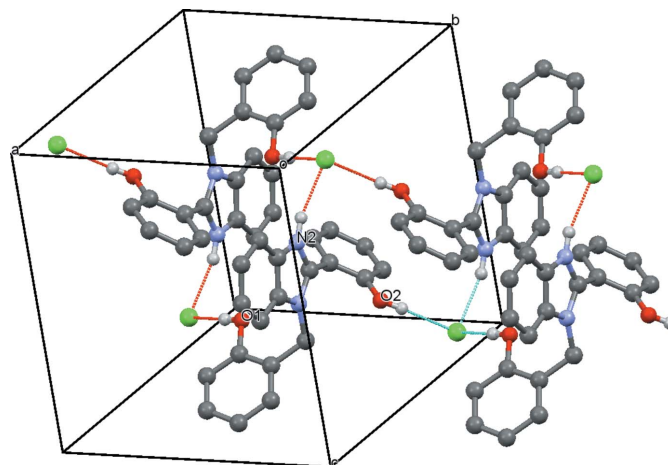


Figure 2
Packing diagram highlighting the hydrogen-bonding interactions.

Table 2

Comparison of notable bond lengths and torsion angles (\AA , $^\circ$).

	Crystal	DFT optimized
C20–O2	1.356 (2)	1.315
C20–C19	1.391 (3)	1.413
C14–N2	1.337 (2)	1.356
C14–N1	1.344 (2)	1.349
\angle C16–C15–C14–N1	123.4 (2)	137.99
\angle C20–C15–C14–N2	125.5 (2)	132.45

observed in the crystal structure within the range of 0.04 \AA (Table 2). The largest distinction between the calculated and crystallographic geometries is related to the twist of the phenolic group attached to the benzimidazole ring system at position 2: in the crystal, the corresponding torsion angles are by 7–14 $^\circ$ nearer to 180 $^\circ$ than the calculated values (Table 2). This could be due to the hydrogen-bonding and C–H $\cdots\pi$ interactions. The ionic nature of the optimized cation–anion pair is reflected in the large calculated dipole moment of 18.05 D. The time-dependent DFT (TD–DFT) calculation was performed on the crystal geometry at the same level of theory as for geometry optimization.

6. UV spectra

The solid-state diffuse reflectance spectrum was measured with a Shimadzu-3600 spectrophotometer fitted with an MPC-3100 sample compartment. For that, the crystals were crushed to powder and mixed with BaSO₄ to a final concentration of 5% (v/v). The Kubelka–Munk transformation (Kubelka & Munk, 1931) was applied to the reflectance data. The spectrum of methanol solution was measured with JASCO V530 spectrophotometer. The solid-state spectrum closely resembles the spectrum of the solution, thus indicating that the geometry and electronic structure of the cation did not change in moving from solid state to solution. In the UV region, the title

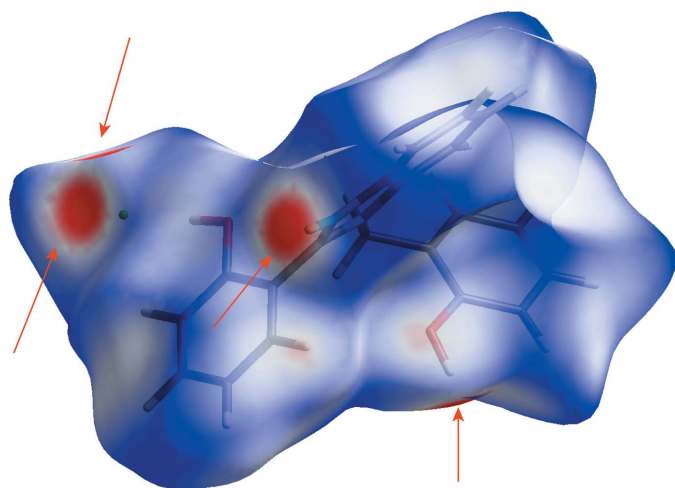


Figure 3

Hirshfeld surface of the ionic pair mapped with normalized contact distances (d_{norm}) indicated by red spots. Positions of close contacts are highlighted by red arrows.

Table 3

Prominent electronic transitions obtained from TD–DFT calculation.

Wavelength	Oscillator strength	Transition
356 nm	0.088	LUMO \leftarrow HOMO-3 (98%)
277 nm	0.2827	LUMO \leftarrow HOMO-5 (96%)
253 nm	0.0537	LUMO+2 \leftarrow HOMO-3 (78%)
		LUMO+3 \leftarrow HOMO-3 (12%)

compound exhibits an absorption maximum at 280 nm and a shoulder around 320 nm (Fig. 4a). The absorption maximum at 280 nm is typical of benzimidazole (Hirayama, 1967), and the 320 nm shoulder is typical of benzimidazole derivatives (Mosquera *et al.*, 1996; Konoshima *et al.*, 2012). The Kubelka–Munk transformed spectrum of the solid sample is quite close to that of a structurally similar derivative reported earlier

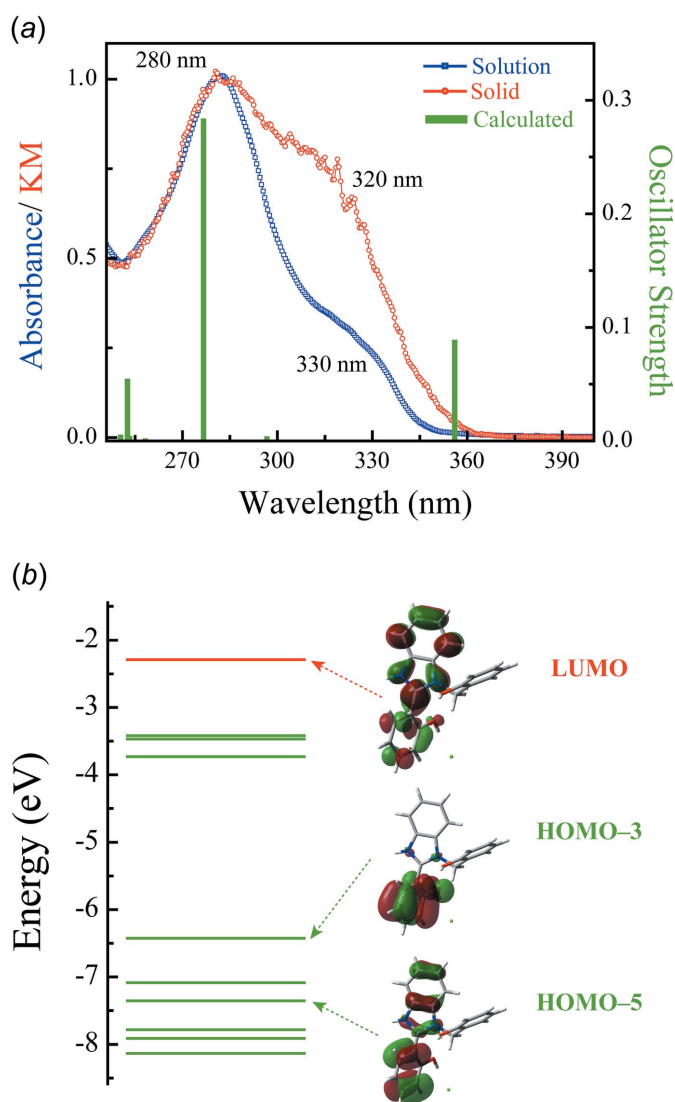


Figure 4

(a) Peak-normalized absorption spectrum of the compound in methanolic solution (blue), Kubelka–Munk (KM) transformed diffuse reflectance solid-state spectrum (red) and TD–DFT calculated transitions (green). (b) Molecular orbital energy levels and the relevant Kohn–Sham orbitals.

(Shida *et al.*, 2013). The positions and intensities of calculated transitions agree well with the experimental data (Fig. 4a, Table 3). The transition at 277 nm is found to have the π - π^* nature. The associated molecular orbitals (HOMO-5 and LUMO) are spread over benzimidazole and 2-phenyl group (Fig. 4b, Table 3). On the other hand, HOMO-3 is localized on 2-phenyl group, making the transitions at 356 nm partially charge-transfer in nature.

7. Database survey

A survey of Cambridge Structure Database (CSD version 5.36, November 2016) (Groom *et al.*, 2016) for molecules with the 2-[1-(2-hydroxybenzyl)-1*H*-benzo[*d*]imidazol-2-yl]phenol skeleton gave 18 hits. All of them are neutral molecules. Among them are an *o*-methylated derivative of the title compound (VIRZEC; Tarte *et al.*, 2007), an *o*-ethoxy derivative (ZARFEF; Ha) , *o*-methoxy derivatives (VOQVAZ and VOQRUP; Al-Douh *et al.*, 2009a and Ha, 2012, respectively). Halide derivatives (C1QOJ, NEGRIB) have also been reported (Fang *et al.*, 2007; Yang *et al.*, 2006). A search for protonated molecules containing the 1-benzyl-2-phenyl-1*H*-benzo[*d*]imidazol-3-ium skeleton gave 11 hits, three of which being closely related to this work are reported in the same article (EBOHOU, EBOHUA and EBOJAI; Wang *et al.*, 2011).

8. Synthesis and crystallization

Salicylaldehyde (SD Fine Chemicals, Mumbai, India), *o*-phenylenediamine (Sigma–Aldrich, USA) and trimethylsilyl chloride (Sigma–Aldrich, USA) were used as received. The title compound was synthesized by the reaction of *o*-phenylenediamine (1 g) with salicylaldehyde (1:2 mole ratio) in double distilled water at 363 K using trimethylsilyl chloride as catalyst (1:1 molar ratio with respect to *o*-phenylenediamine) for 8–10 h (Wan *et al.*, 2009). The reaction mixture was cooled to room temperature, and the white precipitate was filtered off, washed with water, dried by pressing against filter paper and allowed to dry at ambient conditions over a few days. Unexpectedly, the product turned out to be a salt, not a neutral compound, as prescribed by the literature synthetic procedure. It was crystallized from a solution in acetonitrile/methanol mixture (15:85) in a refrigerator and then at room temperature. The resulting plate-shaped crystals were used for single crystal XRD measurements. Even after repeated attempts with crude and recrystallized samples, a clean ¹H NMR spectrum, which is an indication of rotamerism in solution, was not obtained. For the spectroscopic study, the parent solvent was decanted and then the crystals were washed with diethyl ether and finally air dried.

9. Refinement

Crystal data, data collection and structure refinement details are summarized in Table 4. All H atoms were positioned geometrically (O–H = 0.84, N–H = 0.88, C–H = 0.95–

Table 4
Experimental details.

Crystal data	
Chemical formula	C ₂₀ H ₁₇ N ₂ O ₂ ⁺ ·Cl [−]
<i>M_r</i>	352.80
Crystal system, space group	Triclinic, <i>P</i> $\bar{1}$
Temperature (K)	150
<i>a</i> , <i>b</i> , <i>c</i> (Å)	9.8002 (4), 10.6791 (5), 10.6986 (4)
α , β , γ (°)	111.364 (4), 102.346 (3), 111.311 (4)
<i>V</i> (Å ³)	890.75 (7)
<i>Z</i>	2
Radiation type	Mo <i>K</i> α
μ (mm ^{−1})	0.23
Crystal size (mm)	0.19 × 0.18 × 0.12
Data collection	
Diffractometer	Rigaku Saturn 724
Absorption correction	Multi-scan (<i>CrysAlis PRO</i> ; Rigaku Oxford Diffraction, 2015)
<i>T_{min}</i> , <i>T_{max}</i>	0.657, 1.000
No. of measured, independent and observed [<i>I</i> > 2 σ (<i>I</i>)] reflections	8813, 3114, 2654
<i>R_{int}</i>	0.033
(<i>sin</i> θ / λ) _{max} (Å ^{−1})	0.595
Refinement	
<i>R</i> [<i>F</i> ² > 2 σ (<i>F</i> ²)], <i>wR</i> (<i>F</i> ²), <i>S</i>	0.039, 0.105, 1.04
No. of reflections	3114
No. of parameters	228
H-atom treatment	H-atom parameters constrained
$\Delta\rho_{max}$, $\Delta\rho_{min}$ (e Å ^{−3})	0.25, −0.21

Computer programs: *CrysAlis PRO* (Rigaku Oxford Diffraction, 2015), *SHELXT* (Sheldrick, 2015a), *SHELXL2014* (Sheldrick, 2015b) and *OLEX2* (Dolomanov *et al.*, 2009).

0.99 Å) and refined using a riding model with *U*_{iso}(H) = 1.2*U*_{eq}(C,N) [1.5*U*_{eq}(O)]. OH groups were allowed to rotate about the C–bonds.

Acknowledgements

TK thanks the CSIR and IRCC, IIT Bombay for a research fellowship. Department of Chemistry, IIT Bombay is acknowledged for the high-performance computing facility and single-crystal X-ray facility. The authors thank Archit Sanadhya, Harit Kumar and Pooja S. Varak for their efforts in synthesizing the title compound and also thank Shefali Vaidya for her help in drawing the packing diagram.

Funding information

Funding for this research was provided by: Science and Engineering Research Board (grant to Anindya Datta).

References

- Al-Douh, M. H., Osman, H., Hamid, S. A., Kia, R. & Fun, H.-K. (2009a). *Acta Cryst.* **E65**, o925–o926.
- Al-Douh, M. H., Osman, H., Hamid, S. A., Kia, R. & Fun, H.-K. (2009b). *Acta Cryst.* **E65**, o913–o914.
- Benelhadj, K., Massue, J., Retailleau, P., Ulrich, G. & Ziessel, R. (2013). *Org. Lett.* **15**, 2918–2921.
- Carvalho, L. C. R., Fernandes, E. & Marques, M. M. B. (2011). *Chem. Eur. J.* **17**, 12544–12555.
- Dolomanov, O. V., Bourhis, L. J., Gildea, R. J., Howard, J. A. K. & Puschmann, H. (2009). *J. Appl. Cryst.* **42**, 339–341.

- Douhal, A., Amat-Guerri, F., Lillo, M. P. & Acua, A. U. (1994). *J. Photochem. Photobiol. Chem.* **78**, 127–138.
- Fang, X.-N., Liu, L.-M., Huang, G.-S. & Hu, P. (2007). *Acta Cryst.* **E63**, o4881.
- Frisch, M. J., *et al.* (2009). *GAUSSIAN09*. Gaussian Inc., Wallingford, CT, USA.
- Groom, C. R., Bruno, I. J., Lightfoot, M. P. & Ward, S. C. (2016). *Acta Cryst.* **B72**, 171–179.
- Ha, K. (2012). *Acta Cryst.* **E68**, o1398.
- Hirayama, K. (1967). In *Handbook of Ultraviolet and Visible Absorption Spectra of Organic Compounds*. New York: Plenum Press Data Division.
- Keri, R. S., Hiremathad, A., Budagumpi, S. & Nagaraja, B. M. (2015). *Chem. Biol. Drug Des.* **86**, 19–65.
- Konoshima, H., Nagao, S., Kiyota, I., Amimoto, K., Yamamoto, N., Sekine, M., Nakata, M., Furukawa, K. & Sekiya, H. (2012). *Phys. Chem. Chem. Phys.* **14**, 16448–16457.
- Kubelka, P. & Munk, F. (1931). *Z. Tech. Phys.* **11A**, 593–601.
- Mosquera, M., Penedo, J. C., Ríos Rodríguez, M. C. & Rodríguez-Prieto, F. (1996). *J. Phys. Chem.* **100**, 5398–5407.
- Rigaku Oxford Diffraction (2015). *CrysAlis PRO*. Rigaku Oxford Diffraction Ltd, Abingdon, England.
- Ríos Vázquez, S., Ríos Rodríguez, M. C., Mosquera, M. & Rodríguez-Prieto, F. (2008). *J. Phys. Chem. A*, **112**, 376–387.
- Sheldrick, G. M. (2015a). *Acta Cryst.* **A71**, 3–8.
- Sheldrick, G. M. (2015b). *Acta Cryst.* **C71**, 3–8.
- Shida, T., Mutai, T. & Araki, K. (2013). *CrystEngComm*, **15**, 10179–10182.
- Soman, R., Sujatha, S. & Arunkumar, C. (2014). *J. Fluor. Chem.* **163**, 16–22.
- Spackman, M. A. & Jayatilaka, D. (2009). *CrystEngComm*, **11**, 19–32.
- Sun, P., Jian, F. & Tian, Y. (2011). *J. Chem. Crystallogr.* **41**, 1049–1052.
- Tarte, N. H., Cho, H. Y. & Woo, S. I. (2007). *Macromolecules*, **40**, 8162–8167.
- Wan, J.-P., Gan, S.-F., Wu, J.-M. & Pan, Y. (2009). *Green Chem.* **11**, 1633–1637.
- Wang, Y.-T., Tang, G.-M., He, C., Yan, S.-C., Hao, Q.-C., Chen, L., Long, X.-F., Li, T.-D. & Ng, S. W. (2011). *CrystEngComm*, **13**, 6365–6368.
- Yang, X., Jones, R. A., Lai, R. J., Waheed, A., Oye, M. M. & Holmes, A. L. (2006). *Polyhedron*, **25**, 881–887.
- Zhao, D., Hu, J., Wu, N., Huang, X., Qin, X., Lan, J. & You, J. (2011). *Org. Lett.* **13**, 6516–6519.

supporting information

Acta Cryst. (2017). E73, 1143-1147 [https://doi.org/10.1107/S205698901700977X]

Crystal structure and UV spectra of a 1,2-disubstituted benzimidazolium chloride

Tuhin Khan, Navneet Mishra, Darshan S. Mhatre and Anindya Datta

Computing details

Data collection: *CrysAlis PRO* (Rigaku Oxford Diffraction, 2015); cell refinement: *CrysAlis PRO* (Rigaku Oxford Diffraction, 2015); data reduction: *CrysAlis PRO* (Rigaku Oxford Diffraction, 2015); program(s) used to solve structure: SHELXT (Sheldrick, 2015a); program(s) used to refine structure: *SHELXL2014* (Sheldrick, 2015b); molecular graphics: *OLEX2* (Dolomanov *et al.*, 2009); software used to prepare material for publication: *OLEX2* (Dolomanov *et al.*, 2009).

1-(2-Hydroxybenzyl)-2-(2-hydroxyphenyl)-1*H*-benzimidazol-3-ium chloride

Crystal data

$C_{20}H_{17}N_2O_2^+ \cdot Cl^-$
 $M_r = 352.80$
 Triclinic, $P\bar{1}$
 $a = 9.8002$ (4) Å
 $b = 10.6791$ (5) Å
 $c = 10.6986$ (4) Å
 $\alpha = 111.364$ (4)°
 $\beta = 102.346$ (3)°
 $\gamma = 111.311$ (4)°
 $V = 890.75$ (7) Å³

$Z = 2$
 $F(000) = 368$
 $D_x = 1.315$ Mg m⁻³
 Mo $K\alpha$ radiation, $\lambda = 0.71073$ Å
 Cell parameters from 5921 reflections
 $\theta = 2.3$ – 31.1 °
 $\mu = 0.23$ mm⁻¹
 $T = 150$ K
 Plate, colourless
 $0.19 \times 0.18 \times 0.12$ mm

Data collection

Rigaku Saturn 724
 diffractometer
 Radiation source: fine-focus sealed X-ray tube,
 Enhance (Mo) X-ray Source
 Graphite monochromator
 ω scans
 Absorption correction: multi-scan
 (CrysAlis PRO; Rigaku Oxford Diffraction,
 2015)

$T_{\min} = 0.657$, $T_{\max} = 1.000$
 8813 measured reflections
 3114 independent reflections
 2654 reflections with $I > 2\sigma(I)$
 $R_{\text{int}} = 0.033$
 $\theta_{\max} = 25.0$ °, $\theta_{\min} = 2.3$ °
 $h = -11 \rightarrow 10$
 $k = -12 \rightarrow 12$
 $l = -11 \rightarrow 12$

Refinement

Refinement on F^2
 Least-squares matrix: full
 $R[F^2 > 2\sigma(F^2)] = 0.039$
 $wR(F^2) = 0.105$
 $S = 1.04$
 3114 reflections
 228 parameters
 0 restraints

Hydrogen site location: inferred from
 neighbouring sites
 H-atom parameters constrained
 $w = 1/[\sigma^2(F_o^2) + (0.0483P)^2 + 0.2976P]$
 where $P = (F_o^2 + 2F_c^2)/3$
 $(\Delta/\sigma)_{\max} = 0.001$
 $\Delta\rho_{\max} = 0.25$ e Å⁻³
 $\Delta\rho_{\min} = -0.21$ e Å⁻³

Special details

Geometry. All esds (except the esd in the dihedral angle between two l.s. planes) are estimated using the full covariance matrix. The cell esds are taken into account individually in the estimation of esds in distances, angles and torsion angles; correlations between esds in cell parameters are only used when they are defined by crystal symmetry. An approximate (isotropic) treatment of cell esds is used for estimating esds involving l.s. planes.

Refinement. 1. Fixed Uiso At 1.2 times of: All C(H) groups, All C(H,H) groups, All N(H) groups At 1.5 times of: All O(H) groups 2.a Secondary CH2 refined with riding coordinates: C7(H7A,H7B) 2.b Aromatic/amide H refined with riding coordinates: N2(H2A), C2(H2B), C3(H3), C4(H4), C5(H5), C9(H9), C10(H10), C11(H11), C12(H12), C16(H16), C17(H17), C18(H18), C19(H19) 2.c Idealised tetrahedral OH refined as rotating group: O1(H1), O2(H2)

Fractional atomic coordinates and isotropic or equivalent isotropic displacement parameters (\AA^2)

	x	y	z	$U_{\text{iso}}^*/U_{\text{eq}}$
C11	-0.06343 (6)	0.67366 (6)	0.86942 (5)	0.04152 (17)
O1	0.57838 (18)	0.45573 (18)	0.75661 (16)	0.0457 (4)
H1	0.6774	0.5046	0.7816	0.069*
O2	0.07420 (16)	0.49890 (14)	0.68652 (15)	0.0381 (3)
H2	0.0365	0.5481	0.7349	0.057*
N1	0.23361 (18)	0.29524 (16)	0.60618 (15)	0.0302 (3)
N2	0.18508 (19)	0.27540 (17)	0.38883 (16)	0.0337 (4)
H2A	0.1727	0.2994	0.3183	0.040*
C7	0.2833 (2)	0.3651 (2)	0.76670 (19)	0.0325 (4)
H7A	0.1877	0.3293	0.7888	0.039*
H7B	0.3331	0.4783	0.8101	0.039*
C1	0.5475 (2)	0.3725 (2)	0.8279 (2)	0.0355 (4)
C2	0.6572 (3)	0.3358 (2)	0.8901 (2)	0.0428 (5)
H2B	0.7577	0.3671	0.8826	0.051*
C3	0.6179 (3)	0.2535 (2)	0.9626 (2)	0.0467 (5)
H3	0.6913	0.2262	1.0033	0.056*
C4	0.4745 (3)	0.2105 (2)	0.9770 (2)	0.0467 (5)
H4	0.4506	0.1571	1.0303	0.056*
C5	0.3645 (3)	0.2453 (2)	0.9129 (2)	0.0400 (5)
H5	0.2647	0.2148	0.9217	0.048*
C6	0.3999 (2)	0.3248 (2)	0.83576 (18)	0.0325 (4)
C8	0.1953 (2)	0.1454 (2)	0.50925 (19)	0.0321 (4)
C9	0.1862 (2)	0.0217 (2)	0.5291 (2)	0.0380 (5)
H9	0.2058	0.0277	0.6225	0.046*
C10	0.1472 (3)	-0.1105 (2)	0.4064 (2)	0.0428 (5)
H10	0.1417	-0.1968	0.4163	0.051*
C11	0.1156 (3)	-0.1214 (2)	0.2682 (2)	0.0422 (5)
H11	0.0886	-0.2150	0.1867	0.051*
C12	0.1225 (2)	-0.0002 (2)	0.2470 (2)	0.0384 (5)
H12	0.0995	-0.0078	0.1528	0.046*
C13	0.1650 (2)	0.1346 (2)	0.3711 (2)	0.0333 (4)
C14	0.2263 (2)	0.3700 (2)	0.52966 (19)	0.0309 (4)
C15	0.2661 (2)	0.5309 (2)	0.58492 (19)	0.0319 (4)
C16	0.3810 (2)	0.6224 (2)	0.5524 (2)	0.0385 (5)
H16	0.4303	0.5785	0.4957	0.046*

C17	0.4234 (3)	0.7744 (2)	0.6010 (2)	0.0428 (5)
H17	0.5025	0.8362	0.5796	0.051*
C18	0.3493 (3)	0.8366 (2)	0.6819 (2)	0.0402 (5)
H18	0.3796	0.9423	0.7175	0.048*
C19	0.2325 (2)	0.7481 (2)	0.7116 (2)	0.0356 (4)
H19	0.1812	0.7922	0.7651	0.043*
C20	0.1895 (2)	0.5940 (2)	0.66327 (19)	0.0314 (4)

Atomic displacement parameters (Å²)

	U^{11}	U^{22}	U^{33}	U^{12}	U^{13}	U^{23}
C11	0.0437 (3)	0.0520 (3)	0.0327 (3)	0.0275 (3)	0.0155 (2)	0.0196 (2)
O1	0.0415 (9)	0.0639 (10)	0.0441 (8)	0.0290 (8)	0.0202 (7)	0.0329 (8)
O2	0.0398 (8)	0.0354 (7)	0.0450 (8)	0.0232 (7)	0.0205 (7)	0.0183 (6)
N1	0.0339 (9)	0.0275 (8)	0.0257 (8)	0.0183 (7)	0.0072 (7)	0.0089 (6)
N2	0.0394 (10)	0.0352 (8)	0.0272 (8)	0.0214 (8)	0.0109 (7)	0.0139 (7)
C7	0.0370 (11)	0.0326 (10)	0.0250 (9)	0.0199 (9)	0.0095 (8)	0.0099 (8)
C1	0.0420 (12)	0.0379 (10)	0.0254 (9)	0.0232 (9)	0.0114 (9)	0.0117 (8)
C2	0.0449 (13)	0.0488 (12)	0.0330 (11)	0.0305 (11)	0.0106 (10)	0.0131 (9)
C3	0.0574 (15)	0.0436 (12)	0.0340 (11)	0.0329 (11)	0.0055 (10)	0.0127 (10)
C4	0.0639 (16)	0.0346 (11)	0.0321 (11)	0.0226 (11)	0.0068 (11)	0.0154 (9)
C5	0.0452 (13)	0.0335 (10)	0.0313 (10)	0.0161 (9)	0.0094 (9)	0.0126 (9)
C6	0.0401 (11)	0.0295 (9)	0.0217 (9)	0.0192 (9)	0.0073 (8)	0.0070 (8)
C8	0.0312 (11)	0.0289 (9)	0.0292 (10)	0.0172 (8)	0.0066 (8)	0.0079 (8)
C9	0.0400 (12)	0.0343 (10)	0.0343 (10)	0.0206 (9)	0.0074 (9)	0.0131 (9)
C10	0.0435 (13)	0.0312 (10)	0.0451 (12)	0.0222 (10)	0.0078 (10)	0.0117 (9)
C11	0.0391 (12)	0.0329 (10)	0.0366 (11)	0.0190 (9)	0.0069 (9)	0.0027 (9)
C12	0.0364 (12)	0.0385 (11)	0.0278 (10)	0.0192 (9)	0.0064 (9)	0.0067 (8)
C13	0.0291 (10)	0.0337 (10)	0.0317 (10)	0.0178 (9)	0.0079 (8)	0.0106 (8)
C14	0.0293 (10)	0.0332 (10)	0.0291 (9)	0.0187 (8)	0.0084 (8)	0.0123 (8)
C15	0.0339 (11)	0.0327 (10)	0.0278 (9)	0.0195 (9)	0.0072 (8)	0.0130 (8)
C16	0.0437 (12)	0.0436 (11)	0.0380 (11)	0.0276 (10)	0.0184 (10)	0.0216 (9)
C17	0.0440 (13)	0.0415 (11)	0.0499 (12)	0.0220 (10)	0.0189 (11)	0.0274 (10)
C18	0.0467 (13)	0.0311 (10)	0.0404 (11)	0.0203 (10)	0.0094 (10)	0.0181 (9)
C19	0.0418 (12)	0.0365 (10)	0.0326 (10)	0.0262 (10)	0.0113 (9)	0.0157 (9)
C20	0.0313 (10)	0.0340 (10)	0.0278 (9)	0.0178 (9)	0.0073 (8)	0.0145 (8)

Geometric parameters (Å, °)

O1—H1	0.8400	C5—C6	1.393 (3)
O1—C1	1.365 (2)	C8—C9	1.388 (3)
O2—H2	0.8400	C8—C13	1.396 (3)
O2—C20	1.356 (2)	C9—H9	0.9500
N1—C7	1.479 (2)	C9—C10	1.380 (3)
N1—C8	1.402 (2)	C10—H10	0.9500
N1—C14	1.344 (2)	C10—C11	1.396 (3)
N2—H2A	0.8800	C11—H11	0.9500
N2—C13	1.378 (2)	C11—C12	1.374 (3)

N2—C14	1.337 (2)	C12—H12	0.9500
C7—H7A	0.9900	C12—C13	1.394 (2)
C7—H7B	0.9900	C14—C15	1.458 (2)
C7—C6	1.505 (2)	C15—C16	1.400 (3)
C1—C2	1.393 (3)	C15—C20	1.396 (3)
C1—C6	1.381 (3)	C16—H16	0.9500
C2—H2B	0.9500	C16—C17	1.371 (3)
C2—C3	1.380 (3)	C17—H17	0.9500
C3—H3	0.9500	C17—C18	1.385 (3)
C3—C4	1.373 (3)	C18—H18	0.9500
C4—H4	0.9500	C18—C19	1.375 (3)
C4—C5	1.391 (3)	C19—H19	0.9500
C5—H5	0.9500	C19—C20	1.391 (3)
C1—O1—H1	109.5	C10—C9—C8	116.71 (18)
C20—O2—H2	109.5	C10—C9—H9	121.6
C8—N1—C7	126.87 (14)	C9—C10—H10	118.9
C14—N1—C7	124.73 (14)	C9—C10—C11	122.14 (18)
C14—N1—C8	108.30 (14)	C11—C10—H10	118.9
C13—N2—H2A	125.2	C10—C11—H11	119.2
C14—N2—H2A	125.2	C12—C11—C10	121.63 (17)
C14—N2—C13	109.54 (15)	C12—C11—H11	119.2
N1—C7—H7A	109.2	C11—C12—H12	121.8
N1—C7—H7B	109.2	C11—C12—C13	116.42 (18)
N1—C7—C6	112.25 (14)	C13—C12—H12	121.8
H7A—C7—H7B	107.9	N2—C13—C8	106.63 (15)
C6—C7—H7A	109.2	N2—C13—C12	131.29 (17)
C6—C7—H7B	109.2	C12—C13—C8	122.08 (17)
O1—C1—C2	122.67 (19)	N1—C14—C15	128.09 (16)
O1—C1—C6	116.49 (16)	N2—C14—N1	109.17 (15)
C6—C1—C2	120.84 (18)	N2—C14—C15	122.61 (15)
C1—C2—H2B	120.4	C16—C15—C14	118.21 (16)
C3—C2—C1	119.1 (2)	C20—C15—C14	122.35 (17)
C3—C2—H2B	120.4	C20—C15—C16	119.39 (17)
C2—C3—H3	119.5	C15—C16—H16	119.5
C4—C3—C2	121.02 (19)	C17—C16—C15	120.94 (18)
C4—C3—H3	119.5	C17—C16—H16	119.5
C3—C4—H4	120.2	C16—C17—H17	120.5
C3—C4—C5	119.60 (19)	C16—C17—C18	119.01 (19)
C5—C4—H4	120.2	C18—C17—H17	120.5
C4—C5—H5	119.8	C17—C18—H18	119.4
C4—C5—C6	120.3 (2)	C19—C18—C17	121.23 (18)
C6—C5—H5	119.8	C19—C18—H18	119.4
C1—C6—C7	119.68 (16)	C18—C19—H19	120.0
C1—C6—C5	119.00 (18)	C18—C19—C20	120.08 (17)
C5—C6—C7	121.27 (18)	C20—C19—H19	120.0
C9—C8—N1	132.62 (17)	O2—C20—C15	117.13 (16)
C9—C8—C13	121.01 (16)	O2—C20—C19	123.57 (16)

C13—C8—N1	106.36 (15)	C19—C20—C15	119.29 (17)
C8—C9—H9	121.6		
O1—C1—C2—C3	178.87 (18)	C8—C9—C10—C11	-1.1 (3)
O1—C1—C6—C7	0.3 (2)	C9—C8—C13—N2	-179.52 (17)
O1—C1—C6—C5	-177.18 (16)	C9—C8—C13—C12	0.8 (3)
N1—C7—C6—C1	63.1 (2)	C9—C10—C11—C12	0.4 (3)
N1—C7—C6—C5	-119.49 (18)	C10—C11—C12—C13	0.9 (3)
N1—C8—C9—C10	-178.6 (2)	C11—C12—C13—N2	178.91 (19)
N1—C8—C13—N2	-0.2 (2)	C11—C12—C13—C8	-1.5 (3)
N1—C8—C13—C12	-179.86 (17)	C13—N2—C14—N1	-0.2 (2)
N1—C14—C15—C16	123.4 (2)	C13—N2—C14—C15	175.93 (16)
N1—C14—C15—C20	-59.2 (3)	C13—C8—C9—C10	0.5 (3)
N2—C14—C15—C16	-51.9 (3)	C14—N1—C7—C6	-134.04 (18)
N2—C14—C15—C20	125.5 (2)	C14—N1—C8—C9	179.3 (2)
C7—N1—C8—C9	2.7 (3)	C14—N1—C8—C13	0.1 (2)
C7—N1—C8—C13	-176.58 (17)	C14—N2—C13—C8	0.2 (2)
C7—N1—C14—N2	176.79 (16)	C14—N2—C13—C12	179.9 (2)
C7—N1—C14—C15	1.0 (3)	C14—C15—C16—C17	179.90 (18)
C1—C2—C3—C4	-1.4 (3)	C14—C15—C20—O2	-0.1 (3)
C2—C1—C6—C7	-179.56 (16)	C14—C15—C20—C19	-179.40 (17)
C2—C1—C6—C5	3.0 (3)	C15—C16—C17—C18	-0.8 (3)
C2—C3—C4—C5	2.4 (3)	C16—C15—C20—O2	177.20 (16)
C3—C4—C5—C6	-0.6 (3)	C16—C15—C20—C19	-2.1 (3)
C4—C5—C6—C7	-179.43 (17)	C16—C17—C18—C19	-1.2 (3)
C4—C5—C6—C1	-2.0 (3)	C17—C18—C19—C20	1.6 (3)
C6—C1—C2—C3	-1.3 (3)	C18—C19—C20—O2	-179.12 (17)
C8—N1—C7—C6	42.1 (2)	C18—C19—C20—C15	0.1 (3)
C8—N1—C14—N2	0.1 (2)	C20—C15—C16—C17	2.5 (3)
C8—N1—C14—C15	-175.76 (18)		

Hydrogen-bond geometry (\AA , $^\circ$)

<i>D</i> —H \cdots <i>A</i>	<i>D</i> —H	H \cdots <i>A</i>	<i>D</i> \cdots <i>A</i>	<i>D</i> —H \cdots <i>A</i>
O1—H1 \cdots C11 ⁱ	0.84	2.24	3.066 (2)	169
O2—H2 \cdots C11	0.84	2.23	3.071 (1)	177
N2—H2 <i>A</i> \cdots C11 ⁱⁱ	0.88	2.23	3.084 (2)	162
C16—H16 \cdots O1 ⁱⁱⁱ	0.95	2.57	3.253 (2)	129
C19—H19 \cdots C11	0.95	2.93	3.646 (2)	134
C7—H7 <i>B</i> \cdots C <i>g</i> (C1—C6) ^{iv}	0.99	2.77	3.500 (2)	131

Symmetry codes: (i) $x+1, y, z$; (ii) $-x, -y+1, -z+1$; (iii) $-x+1, -y+1, -z+1$; (iv) $-x+1, -y+1, -z+2$.